Use of two-body close-coupling formalisms to calculate three-body breakup cross sections

T. N. Rescigno,[1] C. W. McCurdy,[2] W. A. Isaacs,[2] and M. Baertschy[3]
[1]*Lawrence Livermore National Laboratory, Physics Directorate, Livermore, California 94551*
[2]*Lawrence Berkeley National Laboratory, Computing Sciences, Berkeley, California 94720*
[3]*Department of Applied Science, University of California–Davis, Livermore, California 94550*
(Received 1 June 1999)

We analyze the consequences of discretizing one of the two continua in three-body breakup to reduce it to a two-body close-coupling problem. We identify the origin of oscillations in the singly differential cross section in those ''convergent close-coupling'' calculations as lying only in the way the cross section is calculated from the wave function and not in the wave function itself. The anomalous ''step-function'' behavior of those calculations is derived from a stationary-phase argument. Calculations are presented on the Temkin-Poet model for electron-impact ionization of hydrogen, a breakup problem with exponential potentials, and an analytically solvable model. The anomalies associated with two-body close-coupling calculations are demonstrated using wave functions from complex exterior scaling calculations that otherwise give converged results without any anomalies. [S1050-2947(99)07111-5]

PACS number(s): 34.80.Dp, 03.65.Nk

I. INTRODUCTION

The close-coupling (CC) formalism [1] has been used in electron-scattering calculations for over 40 years, and has formed the basis for most *ab initio* work on low-energy electron-atom scattering. The essence of the method is the use of internal N-electron target states as a basis for expanding the full $(N+1)$-electron wave function. To satisfy the Pauli principle, each term in the expansion is antisymmetrized. Traditionally, close-coupling methods were applied to calculate transitions between discrete states. The target-state expansion must obviously be truncated in actual computations and early applications were limited to the use of a few spectroscopic states. In the late 1960s, it was learned that convergence of excitation cross sections could be accelerated by including positive-energy pseudostates in the expansion [2], typically obtained by diagonalizing the target Hamiltonian in a basis of square-integrable (L^2) functions. When these calculations were extended to energies above the ionization threshold in the early 1970s [3], they were found to encounter problems with unphysical resonances near pseudostate thresholds, but their effects appeared to diminish with increasing number of states [4].

For the close-coupling expansion to ''converge,'' the target states must approach completeness in the interaction region. That this could be realized in a practical calculation was dramatically and convincingly demonstrated for the e-H problem in 1992 by Bray and Stelbovics [5]. By using Laguerre functions to generate discrete target basis sets that could be systematically increased, they showed that the pseudoresonances observed in CC calculations carried out with smaller sets naturally disappear as the basis is increased and that the excitation cross sections converge in this ''convergent close-coupling'' (CCO) scheme. They also showed that the sum of the excitation cross sections into energetically open positive-energy pseudostates gives an accurate representation of the total ionization cross section. This follows from the optical theorem, and the completeness of the target basis: convergence of the elastic scattering amplitude implies convergence of the total cross section. By subtracting the sum of the elastic and excitation cross sections to spectroscopic states from the total cross section, one obtains a convergent approximation to the total ionization cross section. (This same technique was used as early as 1974 by Gallaher [6] to estimate total ionization cross sections with close-coupling calculations that were far from ''convergent.'') Bray and co-workers emphasized that convergence of the total ionization cross section, which is the consequence of using a unitary formalism and a ''complete'' set of discretized target states, says nothing about the way the ionization flux is distributed *within* the continuum [7,8].

Another important step in using close-coupling techniques to calculate ionization phenomena was taken by Konovalov, Bray, and McCarthy in 1994 [9], when they argued that the individual excitation cross sections to positive energy pseudostates calculated in the CCC method could be used to evaluate the singly differential (energy sharing) ionization cross section. It has long been known that the positive energy pseudostates with energies ε_n obtained by diagonalizing the target Hamiltonian in an L^2 basis are, apart from an overall normalization constant, approximately equal to the exact target continuum wave functions at the same energies over the restricted region of coordinate space spanned by the L^2 basis [10]. That being the case, they argued that the corresponding excitation cross sections to such pseudostates should be related to the true singly differential cross section (SDCS) for ejecting a target electron with energy ε_n by a proportionality constant ω_n, that merely reflects the difference in normalization between the pseudostate and the true continuum state. Konovalov, Bray, and McCarthy [9] used the notion of an ''equivalent quadrature'' [11] to argue that the proportionality constant could be approximated as a trapezoidal quadrature weight $\omega_n=(\varepsilon_{n+1}-\varepsilon_{n-1})/2$ [12]. Bray and co-workers [13] later refined this approach by using the overlap integrals between the pseudostates and the true continuum functions to ''renormalize'' the underlying T-matrix elements. The fact that these renormalized amplitudes could be used to compute detailed triply differential ionization cross sections whose

shapes matched experimental data led Bray and Fursa to question whether the CCC method was in fact ''a complete scattering theory'' [14].

Since the electrons are indistinguishable, the singly differential cross section $(d\sigma/d\varepsilon)$ should be symmetric about $E/2$, where E is the energy relative to the ionization threshold, that is, the probability of finding an ejected electron with energy ε should be the same as finding it with energy $E-\varepsilon$, where $0<\varepsilon<E$. This is the symmetrization postulate that emerges in the formal theory [15]. This property does not follow automatically from the close-coupling formalism, even though the underlying wave function is antisymmetric. In the close-coupling treatment, the probabilities of producing ejected electrons with energies ε and $E-\varepsilon$ are connected with independent excitation amplitudes for pseudostates with energies ε and $E-\varepsilon$ and are not related by any specific symmetry relation [16]. Indeed, it was noticed that for these ''raw'' CCC ionization cross sections, those connected with pseudostates whose energies ε were greater than $E/2$ were very much smaller than those for which ε was less than $E/2$ [13]. The required symmetry was restored in the CCC formalism by the artifice of defining a unitarity preserving observable cross section as [9,13,16]

$$\frac{d\sigma(\varepsilon)}{d\varepsilon}=\frac{d\overline{\sigma}(\varepsilon)}{d\varepsilon}+\frac{d\overline{\sigma}(E-\varepsilon)}{d\varepsilon}, \tag{1}$$

where the bars refer to the raw pseudostate excitation cross sections. The total ionization cross section is then given as

$$\sigma^{i}=\int_0^E d\varepsilon\,\frac{d\overline{\sigma}(\varepsilon)}{d\varepsilon}=\int_0^{E/2} d\varepsilon\,\frac{d\sigma(\varepsilon)}{d\varepsilon}. \tag{2}$$

The *ad hoc* idea of expressing the observable ionization cross section as an incoherent sum of cross sections corresponding to two distinguishable processes has been a source of some discussion and has led some [17] to question the validity of the CCC approach to ionization, since it seems to be incompatible with the formal theory of ionization [15]. It is important to mention that the observed asymmetry in the raw excitation cross sections is not peculiar to the CCC approach, and has also been observed in other implementations of the close-coupling method [8].

Bray [18] commented recently on the way the singly differential cross section (SDCS) is evaluated in the CCC method, and tried to reconcile it with the formal theory. He argued that in the limit of an infinite basis the raw excitation cross sections will vanish for $\varepsilon>E/2$, and hence only one of the terms in Eq. (1) will be nonzero. However, if the true SDCS is nonzero at $E/2$, then the CCC method will try to approximate a function that goes to zero discontinuously, and there will be a resulting lack of convergence for any finite basis. This ''step-function hypothesis'' was used to explain the poor convergence in the SDCS found in CCC calculations of e-H ionization at low energies. There is less trouble at higher energies. As the collision energy increases, the value of the ''step'' at $E/2$ in the SDCS decreases, and the cross sections tend to be more strongly peaked near $\varepsilon=0$.

A simplified model of e-H scattering known as the Temkin-Poet model [19], which treats only states of zero angular momentum and replaces the true electron-electron repulsion by its spherical average, has provided a vehicle for testing these ideas numerically and has been the subject of many recent papers on ionization. For the triplet case (total spin 1), the antisymmetry of the wave function requires that the SDCS vanish at the point $\varepsilon=E/2$, and a recent benchmark calculation [20] has verified that the results of the close-coupling calculations appear to be converging to the correct values for $\varepsilon<E/2$. For the singlet case, where the SDCS has a substantial value at $E/2$ for energies below 100 eV, the CC values are found to oscillate about the correct values for $\varepsilon<E/2$. For $\varepsilon>E/2$, the calculations presented in Ref. [20] yield the expected symmetry, while the CC cross sections are near zero.

In assessing the significance of the close-coupling approach to ionization, it is important to bear in mind that the recent applications which treat differential ionization processes do not share the same mathematical foundation that characterized previous close-coupling studies which were limited to calculating total ionization cross sections. The total ionization cross section is related by unitarity to the total and nonbreakup cross sections, and the convergence of the latter is linked to the completeness of the underlying target expansion basis. However, the assertion that the *differential* ionization cross sections computed by the CCC method are correct is based more on empirical evidence (the results seem to agree with available experimental data) than on mathematical rigor. For example, Bray and co-workers argued that the close-coupling method implies a distinguishable electron model of ionization since one electron is in a bound pseudostate and the other in a true continuum state [16,18]. They further argued that since a ''detector'' positioned at ''infinity'' only detects the true continuum electron, it is natural to expect the raw excitation amplitudes corresponding to pseudostates with $\varepsilon>E/2$ to tend to zero, since they correspond to a ''bound'' electron reaching the detector before a completely shielded slow electron in a plane-wave state. It is not clear whether this completely heuristic argument, since it makes reference to shielding, would also apply to close-coupling calculations of breakup processes in situations that only involve short-range interactions.

In a recent paper [20], we presented accurate numerical ionization cross sections for a model three-body Coulomb problem, which were obtained by a method that does not rely on any specific asymptotic form being imposed on the wave function. In our method, we introduce a two-dimensional numerical grid and solve directly for the outgoing-wave part of the full wave function using either finite-element [21] or finite-difference [20] techniques. We avoided the specification of asymptotic boundary conditions by applying an exterior complex scaling transformation [22] to both radial electron coordinates:

$$R(r)=\begin{cases} r, & r<R_0 \\ R_0+(r-R_0)e^{i\phi}, & r\geq R_0 \end{cases}, \tag{3}$$

and extrapolating the results to infinite R_0. In comparing our results with those obtained by two different close-coupling techniques [8], both of which gave nonconvergent results for the singlet case, we speculated that perhaps the oscillations found in the CC results were tied more to the way the ionization information was being extracted than to any inaccu-

racies in the underlying wave functions. Additional evidence that this might indeed be the case is provided by the recent work of Ref. [23] on the Temkin-Poet model. The purpose of this paper is to explore that speculation in some detail. We will present numerical evidence that it is possible to reproduce oscillating structures in differential ionization cross sections similar to those seen in the CC treatments from a wave function that produces entirely stable and correct results (symmetric about $E/2$) when a different technique is used to extract the same information. Moreover, we demonstrate that this curious behavior is not the result of long-range Coulomb interactions. Finally, by a combination of numerical experiments on a model problem and some formal manipulations based on stationary-phase ideas, we attempt to explain the origin of the ''step-function hypothesis'' that was introduced to explain the behavior of the calculated CCC ionization cross sections.

II. DISCRETIZED CONTINUUM STATES IN TWO-BODY CLOSE-COUPLING CALCULATIONS ON BREAKUP

We treat a system of two light particles (electrons) moving in the field of an infinitely massive third body (proton). For simplicity, we ignore angular-momentum effects and assume the Hamiltonian for the system is a function of two radial variables:

$$H=-\frac{1}{2}\frac{d^2}{dr_1^2}-\frac{1}{2}\frac{d^2}{dr_2^2}+V_1(r_1)+V_2(r_2)+V(r_1,r_2). \quad (4)$$

If the two one-body potentials V_1 and V_2 are the same, and $V(r_1,r_2)$ is symmetric under interchange of particles 1 and 2, then the wave functions can be labeled by their parity ($\pm$) under particle exchange. We first partition the full two-particle wave function into unperturbed, $\Psi_0^{\pm}$, and scattered wave, $\Psi_{\rm SC}^{\pm}$, parts. The scattered wave function is defined as [21]

$$\Psi_{\rm sc}^{\pm}=G(E)(H-E)\Psi_0^{\pm}, \quad (5)$$

where $G(E)$ is the full outgoing-wave Green's function. In a close-coupling method, the scattered wave function would be expressed as

$$\Psi_{\rm sc}^{\pm}(r_1,r_2)=\sum_{\alpha}\chi_{\alpha}(r_1)g_{\alpha}(r_2)\pm\chi_{\alpha}(r_2)g_{\alpha}(r_1)+\sum_{\alpha,\beta}c_{\alpha\beta}\chi_{\alpha}(r_1)\chi_{\beta}(r_2), \quad (6)$$

where the states χ_{α} are obtained by diagonalizing the ''target'' Hamiltonian $-\frac{1}{2}d^2/dr_1^2+V_1(r_1)$ in some discrete basis, and the channel functions g_{α} have the asymptotic form (for open channels)

$$g_{\alpha}(r)\underset{r\to\infty}{\to}T_{0\to\alpha}e^{ik_{\alpha}r}/\sqrt{k_{\alpha}}, \quad (7)$$

where k_{α} is the channel momentum, and $T_{0\to\alpha}$ is a two-body T-matrix element (scattering amplitude). The channel functions are assumed to be orthogonal to the target states, so we compensate for this orthogonality constraint by including the second sum on the right-hand side of Eq. (6).

Close-coupling calculations are typically carried out with target states that are generated in a discrete basis of functions that are orthogonal on $[0,\infty]$. However, since we will be carrying out experiments with wave functions that are generated on a finite two-dimensional mesh of grid points, it is more convenient to use basis functions that are orthogonal on a finite interval $[0,L]$. In this work, we use a so-called discrete variable representation (DVR) [24] and choose a set of Lagrange-mesh functions

$$u_i(r)=\prod_{j\neq i}\frac{r-r_j}{r_i-r_j} \quad (8)$$

as our basis functions. Note that these functions have the property

$$u_i(r_j)=\delta_{i,j}. \quad (9)$$

The mesh points we use, $\{r_i, i=0,...,N+1\}$, are connected to a Gauss quadrature rule. Specifically, the mesh points are chosen to be Gauss-Lobatto quadrature points on the interval $[0,L]$. The Gauss-Lobatto quadrature is similar to the more familiar Gauss-Legendre quadrature, the difference being that the quadrature points must include the two end points 0 and L. This property makes it easy to impose physical boundary conditions. Equations (8) and (9) show that the only basis functions that are nonzero at the end points of the interval are u_0 and u_{N+1}, so by excluding these two functions from the basis we can generate a set of box-normalized target states that vanish at the end points. Manolopoulos and Wyatt [25] were the first to use this particular DVR basis, which they called *Lobatto shape functions*, in scattering calculations and we refer the interested reader to their work for additional details. The use of a DVR trivializes the calculation of the Hamiltonian matrix elements, if the underlying Gauss quadrature rule is used. Moreover, since the basis is connected to a classical Gauss quadrature, it can be systematically increased toward completeness (on $[0,L]$) without posing any numerical difficulties.

III. CALCULATIONS IN THE TEMKIN-POET MODEL

The first set of calculations we describe use Temkin-Poet wave functions, $\Psi_{\rm sc}^{\pm}(r_1,r_2)$, at total energy $E=1.0$ hartree that were obtained from an earlier study in which the scattered wave equation (5), was solved by a high-order finite-difference scheme on a complex, exterior-scaled, two-dimensional grid [20]. The real part of the grid extended out to 200 bohr in both r_1 and r_2, and on the complex portions of the grid beyond that value the Coulomb potentials were truncated to assure an exponential decrease in the wave function on the scaled portions of the grid. To decompose this wave function into two-body components, we have to choose a basis whose range lies within the portion of the grid where both coordinates are real. A set of single-particle target functions χ_n, was generated by diagonalizing the s-wave radial hydrogen Hamiltonian in a DVR basis of 100 Lobatto shape functions in a box of length 90.0 bohr. The basis produces eight negative-energy target states and 33 positive-energy states below 1.0 hartree. The scattered wave function was

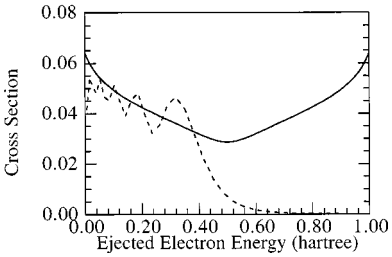

FIG. 1. Singlet SDCS (units of πa_0^2/hartree) for the Temkin-Poet model at 40.82-eV incident energy. Solid line: exterior complex scaling calculations; dashed line: projection onto the two-body close-coupling representation.

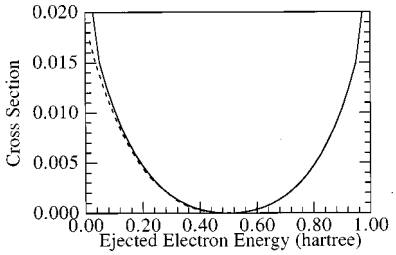

FIG. 2. Triplet SDCS (units of πa_0^2/hartree) for the Temkin-Poet model at 40.82-eV incident energy. Solid line: exterior complex scaling calculations; dashed line: projection onto the two-body close-coupling representation.

interpolated onto the grid of DVR points. Assuming the scattered wave function can be expanded as in Eq. (6), we numerically projected the wave function onto open target states and evaluated the resulting one-particle function at the point $r_2=L$:

$$g_n(L)=\int_0^L dr_1 \chi_n(r_1)\Psi_{\rm sc}^{\pm}(r_1,L)\equiv A_n T_{0\to n} e^{ik_n L}/\sqrt{k_n}, \quad (10)$$

where A_n is a constant related to the normalization of the target state. The ''cross sections'' are evaluated from the so defined T-matrix elements. For bound target states, the cross sections are obtained directly from the T-matrix elements given by Eq. (10). We checked that the elastic, $2s$, and $3s$ excitation cross sections computed in this fashion agreed with values reported by others [26]. For the positive-energy pseudostates, we have to restore the proper continuum density of states to the excitation cross sections. Adopting the procedure of Konovalov, Bray, and McCarthy [9], we assume that the pseudostates give a discretization of the continuum that can be interpreted as an energy quadrature:

$$\sum_{0<\varepsilon_n<E} |\chi_n\rangle\langle\chi_n| = \int_0^E d\varepsilon |\varepsilon\rangle\langle\varepsilon| \approx \sum_{0<\varepsilon_n<E} \omega_n |\varepsilon_n\rangle\langle\varepsilon_n|, \quad (11)$$

where $|\chi_n\rangle$ is a pseudostate and $|\varepsilon_n\rangle$ is an exact target continuum state at the same energy. To compute the SDCS we therefore divide the cross sections computed from Eq. (10) by the appropriate weight ω_n, which identifies the constant A_n as $\sqrt{\omega_n}$. We used the trapezoidal rule formula for the quadrature weights given by Bransden and Stelbovics [12]:

$$\omega_n=(\varepsilon_{n+1}-\varepsilon_{n-1})/2, \quad n\neq 1,M,$$
$$\omega_1=(\omega_1+\omega_2)/2, \quad (12)$$
$$\omega_M=E-(\varepsilon_M+\varepsilon_{M-1})/2,$$

where $0\leqslant\varepsilon_1,\ldots,\varepsilon_M\leqslant E$. The renormalized excitation cross sections to the open positive-energy target states are plotted in Figs. 1 and 2 for the singlet and triplet cases, respectively. These curves bear a strikingly similar resemblance to the results found in the close-coupling treatments [8]. The triplet cross sections so computed accurately follow what we know to be the correct SDCS for target state energies up to $E/2$; beyond that point, they become vanishingly small. The singlet cross sections appear to oscillate about the correct values before becoming small for energies greater than $E/2$.

It is important to bear in mind that this behavior is not a reflection of any inherent errors in the wave functions we started with, but rather appears to be the result of the particular way in which the SDCS is being ''extracted.'' The wave functions we are using have the proper symmetry under interchange of r_1 and r_2. Indeed, if we use hyperspherical coordinates $\rho=\sqrt{r_1^2+r_2^2}$ and $\alpha=\tan^{-1}(r_1/r_2)$ to express the differential ionization cross section in terms of the flux due to $\Psi_{\rm sc}^{\pm}(r_1,r_2)$ through a hypersphere of radius ρ_0 [15],

$$\mathbf{F}(\rho_0,\alpha)=\frac{1}{2i}\left[(\Psi_{\rm sc}^{\pm})^*\nabla\Psi_{\rm sc}^{\pm}-\Psi_{\rm sc}^{\pm}\nabla(\Psi_{\rm sc}^{\pm})^*\right]\big|_{\rho=\rho_0} \quad (13)$$

then for large ρ_0 we can identify α as $\tan^{-1}(k_1/k_2)$, and compute the SDCS from the expression

$$\frac{d\sigma(\varepsilon)}{d\varepsilon}=\frac{1}{E\sin\alpha\cos\alpha}\frac{4\pi}{k_0^2}\mathbf{F}(\rho_0,\alpha)\cdot\rho_0, \quad (14)$$

where $k_0^2/2$ is the incident electron energy. This latter procedure gives the smooth curves shown in the figures that are fully consistent with the symmetrization postulate.

IV. CALCULATIONS OF BREAKUP CROSS SECTIONS FOR SHORT-RANGE POTENTIALS

Having established that we can reproduce the structures found in other CC calculations of differential ionization cross sections in the Temkin-Poet model, we can now question whether the observed behavior was peculiar to problems involving Coulomb interactions or whether it would be found in other cases as well. In formulating the ''step-function hypothesis,'' Bray argued that the excitation cross sections to positive-energy pseudostates with $\varepsilon>E/2$ should tend to zero in the limit of a complete target basis, because they represent the unphysical situation in which a ''bound'' electron reaches the detector before a completely shielded slow electron in a plane-wave state. Does this argument hinge on any shielding of the ''free'' electron from the Coulomb interaction with the proton?

We performed a second set of calculations with short-range potentials, choosing the Hamiltonian

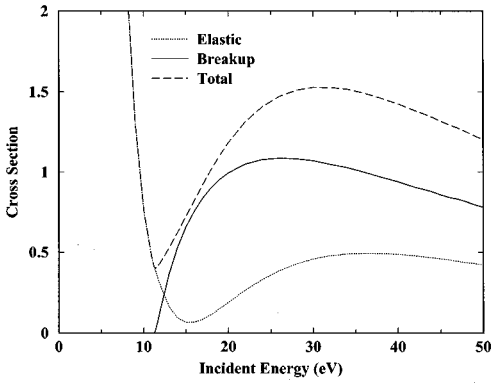

FIG. 3. Cross sections (in units of a_0^2) for the short-range potential problem defined in the text. Dashed line: total scattering; solid line: breakup; dotted line: elastic scattering.

$$H=-\frac{1}{2}\frac{d^2}{dr_1^2}-\frac{1}{2}\frac{d^2}{dr_2^2}-3e^{-r_1}-3e^{-r_2}+10e^{-(r_1+r_2)}. \tag{15}$$

The one-particle Hamiltonian has a single bound state with energy -11.19 eV. We performed calculations on this system using a finite element basis like that used in some of our earlier calculations on ionization that employed exterior complex scaling [21]. This calculation employed a two-dimensional grid whose real part extended to 40.0 bohr, and whose complex part extended to 60.0 bohr.

Figure 3 shows the total, elastic, and integral breakup cross sections for this problem for singlet coupling. This problem makes a convenient test case, since for this choice of potential parameters the breakup cross section is as large as or larger than the elastic-scattering cross section from threshold to 50.0 eV. Because the target binds only one state, the only processes allowed are elastic scattering and breakup. Evidently because the repulsive potential between the electrons is of such short range, the analogous triplet breakup cross section is as much as an order of magnitude or more smaller in this energy range.

We generated the scattered wave function at an incident energy of 24.0 eV on a numerical grid, and computed the singly differential breakup cross section by computing the flux directly using Eqs. (13) and (14) in exactly the same way used in our previous calculations on ionization [20,27]. That SDCS, shown in Fig. 4, is a smooth curve and satisfies the symmetrization postulate. We then decomposed this same wave function into two-body components, and computed the SDCS by the method described in Sec. III. For the single-particle states, we also chose a box of length 40.0 bohr, but this time used a basis of 50 DVR Lobatto functions, which produced 12 energetically open pseudostates at the specified total energy. The SDCS values obtained by projecting the scattered wave onto target states is also shown in Fig. 4. The results behave exactly as they did in the Temkin-Poet case, arguing strongly that the observed behavior is linked to the method of extraction of the SDCS from the wave function, and has nothing to do with the Coulomb potentials of the atomic ionization problem. Note that the *total* breakup cross section, obtained by summing the two-body excitation cross sections, was found to be $1.03a_0^2$, in good agreement with the value $1.06a_0^2$ obtained from the flux calculation.

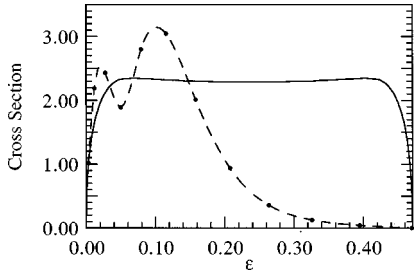

FIG. 4. SDCS (in units of a_0^2/hartree) at 24.0-eV incident energy for the short-range potential problem as a function of ejection energy (hartree). Solid line: exterior complex scaling; dashed line: projection onto the two-body close-coupling representation.

V. ANALYTICALLY SOLVABLE TEST PROBLEM

While the foregoing numerical experiments give convincing evidence that the representation of the wave function in terms of a close-coupling expansion is responsible for the observed behavior in the extracted SDCS, they unfortunately shed little light on any underlying mathematical reasons for such a curious result. To gain further insight, we now turn to a simple model problem that has an analytical solution. We consider a hypothetical breakup problem in which the free-particle Green's function governs the motion of the scattered wave. Consider first the Green's function for two free particles defined by the equation

$$[E+\tfrac{1}{2}\nabla_1^2+\tfrac{1}{2}\nabla_2^2]G(\mathbf{r_1},\mathbf{r_2};\mathbf{r_1'},\mathbf{r_2'};E)=\delta(\mathbf{r_1}-\mathbf{r_1'})\,\delta(\mathbf{r_2}-\mathbf{r_2'}). \tag{16}$$

The outgoing-wave solution for this problem can be expressed in a closed form as [28]

$$G(\mathbf{r_1},\mathbf{r_2};\mathbf{r_1'},\mathbf{r_2'};E)=-\frac{i}{4\pi^2}\frac{H_2^{(1)}(K|\rho-\rho'|)}{|\rho-\rho'|^2}, \tag{17}$$

where $E=K^2/2$, $H_2^{(1)}$ is a Hankel function of integer order 2, and ρ is the 6-vector:

$$\rho=\begin{bmatrix}\mathbf{r_1}\\ \mathbf{r_2}\end{bmatrix}. \tag{18}$$

We want the Green's function for s waves, which is obtained from Eq. (17) by taking the matrix element

$$\frac{G(r_1,r_2;r_1',r_2';E)}{r_1r_2r_1'r_2'}=\int Y_{00}^*(\Omega_1)Y_{00}^*(\Omega_2)G(\mathbf{r_1},\mathbf{r_2};\mathbf{r_1'},\mathbf{r_2'};E)\times Y_{00}(\Omega_1')Y_{00}(\Omega_2')d\Omega_1d\Omega_2d\Omega_1'd\Omega_2'. \tag{19}$$

The integrations can be performed by using the identity

$$\frac{\partial\partial}{\partial x\partial y}H_0^{(1)}((a-bx-cy)^{1/2})=bc\frac{H_2^{(1)}((a-bx-cy)^{1/2})}{4(a-bx-cy)} \tag{20}$$

to derive the result

$$G(r_1,r_2;r_1',r_2';E)=-\frac{i}{2}\{H_0^{(1)}[K((r_1^2+r_1'^2)+(r_2^2+r_2'^2))^{1/2}]-H_0^{(1)}[K((r_1^2-r_1'^2)+(r_2^2+r_2'^2))^{1/2}]-H_0^{(1)}[K((r_1^2+r_1'^2)+(r_2^2-r_2'^2))^{1/2}]+H_0^{(1)}[K((r_1^2-r_1'^2)+(r_2^2-r_2'^2))^{1/2}]\}. \quad (21)$$

If we switch to hyperspherical coordinates, $r_1=\rho\sin\alpha$ and $r_2=\rho\cos\alpha$, and use the asymptotic form of the Hankel function,

$$H_0^{(1)}(z)\rightarrow e^{-i\pi/4}\left(\frac{2}{\pi}\right)^{1/2}\frac{e^{iz}}{z^{1/2}}, \quad (22)$$

we obtain the limiting behavior of $G(r_1,r_2;r_1',r_2';E)$ for large ρ:

$$G(r_1,r_2;r_1',r_2';E)\underset{\rho\rightarrow\infty}{\rightarrow}-e^{-i3\pi/4}2\left(\frac{2}{\pi}\right)^{1/2}\times\frac{e^{iK\rho}}{(K\rho)^{1/2}}\sin(K\sin(\alpha)r_1')\sin(K\cos(\alpha)r_2'). \quad (23)$$

We now consider a hypothetical problem in which the scattered wave is determined by the equation

$$\left(E+\frac{1}{2}\frac{d^2}{dr_1^2}+\frac{1}{2}\frac{d^2}{dr_2^2}\right)\Phi(r_1,r_2)=\phi_0(r_1,r_2) \quad (24)$$

or

$$\Phi(r_1,r_2)=\int\int G(r_1,r_2;r_1',r_2';E)\phi_0(r_1',r_2')dr_1'dr_2', \quad (25)$$

where $\phi_0(r_1,r_2)$ is an arbitrary short-range source term. We chose the latter to be a simple product of exponentials:

$$\phi_0(r_1,r_2)=e^{-ar_1}e^{-br_2}. \quad (26)$$

With this choice, we can use the asymptotic form for G given in Eq. (23) to perform the integration in Eq. (25) analytically, and obtain an expression for $\Phi(r_1,r_2)$ which is valid for large ρ:

$$\Phi(r_1,r_2)\underset{\rho\rightarrow\infty}{\rightarrow}-e^{-i3\pi/4}2\left(\frac{2}{\pi}\right)^{1/2}\frac{e^{iK\rho}}{(K\rho)^{1/2}}\times\left(\frac{K\sin\alpha}{a^2+K^2\sin^2\alpha}\right)\left(\frac{K\cos\alpha}{b^2+K^2\cos^2\alpha}\right). \quad (27)$$

We can thus define a differential breakup amplitude for this simple model as

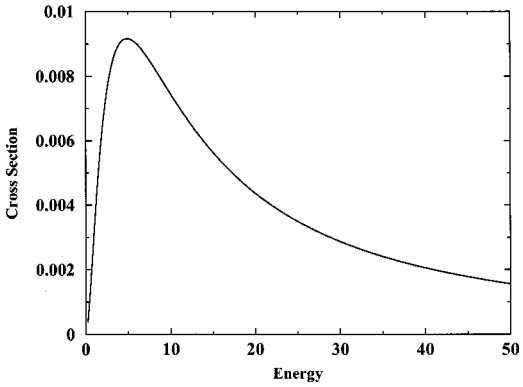

FIG. 5. Total breakup cross section (in units of a_0^2) as a function of energy (in eV) for the analytically solvable model defined in the text.

$$f(\alpha)=-e^{-i3\pi/4}2\left(\frac{2}{\pi}\right)^{1/2}\left(\frac{K\sin\alpha}{a^2+K^2\cos^2\alpha}\right)\left(\frac{K\cos\alpha}{b^2+K^2\sin^2\alpha}\right), \quad (28)$$

with the corresponding SDCS

$$\frac{d\sigma}{d\varepsilon}=\frac{1}{k_1k_2}|(\alpha)|^2, \quad (29)$$

where $\varepsilon=k_1^2/2$, $\alpha=\tan^{-1}(k_1/k_2)$, and $K^2=k_1^2+k_2^2$. The integral cross section corresponding to this SDCS,

$$\sigma(E)=\int_0^E\frac{d\sigma}{d\varepsilon}\,d\varepsilon, \quad (30)$$

is plotted in Fig. 5, and qualitatively resembles that for ionization of an atom. The SDCS as a function of ε is plotted in Fig. 6 for the case $K=4$ with $a=b=2$. It resembles the SDCS for the short-range potential problem of Sec. IV.

To obtain a representation of the SDCS in terms of one-body ''target'' states for this problem, we use particle in a box functions normalized on $[0,L]$:

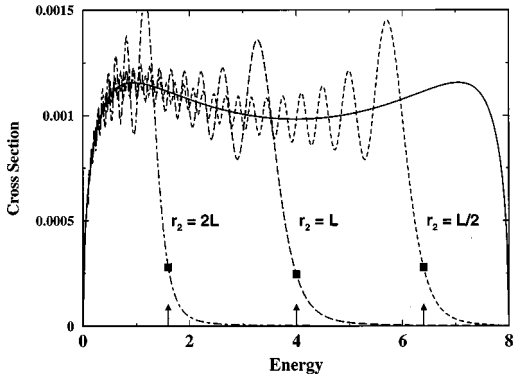

FIG. 6. SDCS (in units of a_0^2/hartree) as a function of ejection energy (hartree) for the analytically solvable model. The solid curve is the exact value, and the broken curves are the results of projection with different values of r_2. The solid squares are the points at which the stationary-phase formula predicts the projected SDCS to be one-fourth of the correct answer.

$$\chi_n(r_1)=\left(\frac{2}{L}\right)^{1/2}\sin(k_n r_1),\quad k_n=\frac{n\pi}{L}, \tag{31}$$

with the corresponding continuum quadrature weights

$$\omega_n=\frac{1}{2}\,({k_{n+1}}^2/2-{k_{n-1}}^2/2)=\frac{\pi}{L}\,k_n\,. \tag{32}$$

To obtain ''close-coupling'' representation of the SDCS, $d\sigma^{CC}/d\varepsilon_n$, we fix the value of r_2 in Eq. (25), multiply by $\chi_n(r_1)$, and numerically integrate over r_1. The computation can be simplified by using the momentum-space representation of the free-particle Green's function:

$$\begin{aligned}G(r_1,r_2;r_1',r_2';E)&=\frac{4}{\pi^2}\int_0^\infty dq_1\int_0^\infty dq_2\\&\times\frac{\sin(q_1r_1)\sin(q_2r_2)\sin(q_1r_1')\sin(q_2r_2')}{E-q_1^2/2-q_2^2/2+i\eta}.\end{aligned} \tag{33}$$

Using this representation in the projection on the one-body ''target'' states,

$$\begin{aligned}g_n(r_2)&=\int_0^L\chi_n(r_1)\Phi(r_1,r_2)dr_1\\&=\int_0^L\chi_n(r_1)\int\int G(r_1,r_2;r_1',r_2';E)\phi_0(r_1',r_2')\\&\times dr_1'dr_2'dr_1,\end{aligned} \tag{34}$$

allows us to do the integrals over r_1', r_2', and r_1 analytically because they involve only products of trigonometric functions and exponentials. Moreover the integral over q_2 can then be done by contour integration after some observations about symmetries in the integrand have been made that allow the range of integration to be extended over the entire real axis. The result is an expression for the results of the projection in terms of a single quadrature over q_1, which can be performed numerically:

$$\begin{aligned}g_n(r_2)&=\frac{2i}{\pi}\left(\frac{2}{L}\right)^{1/2}\int_{-\infty}^{\infty}dq_1\frac{q_1}{(a^2+q_1^2)(k_n^2-q_1^2)(K^2+b^2-q_1^2)}\\&\times(e^{ir_2\sqrt{K^2-q_1^2}}-e^{-br_2})[k_n-e^{iq_1L}(k_n\cos(k_nL)\\&-iq_1\sin(k_nL))].\end{aligned} \tag{35}$$

As in Eq. (10), identifying the ionization amplitude as the coefficient of $e^{ik_nr_2}/\sqrt{k_n}$ in the large-r_2 limit, where $K^2=k_n^2+p_n^2$, we evaluate the cross section as

$$\frac{d\sigma^{cc}}{d\varepsilon_n}=\frac{1}{\omega_n}\,|g_n(r_2)e^{-ip_nr_2}\sqrt{p_n}|^2. \tag{36}$$

In Fig. 6, we compare this representation with the ''exact'' SDCS given in Eqs. (28) and (29). For these calculations, we chose $L=100$. To see how the results depend on the value chosen for r_2 in Eq. (34), we plot the SDCS for three different choices $r_2=50.$, 100. and 200. Once again we find that the CC representation give values that oscillate about the correct results for small k_n. However, we now find that the energy beyond which the cross section effectively vanishes depends on the value of r_2 that was used in the extraction. When $r_2=L$, the cross sections are small for $\varepsilon_n>E/2$. However, this point can be shifted to higher or lower values of ε_n by choosing values of r_2 less than or greater than that of L, respectively. The behavior seen in Fig. 6 is found for other values of L as well; as the value of L is increased, the magnitude of the oscillations about the correct values decreases, but the point at which the SDCS vanishes only depends on the ratio of r_2 to L. Understanding this behavior is the key to explaining the ''step-function hypothesis.''

VI. STATIONARY-PHASE DERIVATION OF ''STEP-FUNCTION HYPOTHESIS''

The fact that r_2 is large in Eq. (31) suggests that the CC cross section can be evaluated using the stationary-phase approximation [29], which approximates integrals of the form

$$I\equiv\int_0^L\phi(x)e^{i\lambda g(x)}dx\underset{\lambda\to\infty}{=}\begin{cases}\left(\dfrac{2\pi}{\lambda g''(x_0)}\right)^{1/2}\phi(x_0)e^{i(\lambda g(x_0)+\pi/4)}, & g'(x_0)=0,\quad 0<x_0<L\\ \left(\dfrac{\pi}{2\lambda g''(x_0)}\right)^{1/2}\phi(x_0)e^{i(\lambda g(x_0)+\pi/4)}, & g'(x_0)=0,\quad x_0=L\\ 0, & g'(x)\neq,\quad 0\leqslant x_0\leqslant L.\end{cases} \tag{37}$$

The integral we want to consider is

$$I_n=\sqrt{2/L}\int_0^L dr_1\sin(k_nr_1)f(K,\alpha)e^{iK\rho}/\sqrt{K\rho}. \tag{38}$$

Writing $\sin(k_nr_1)$ as $(e^{ik_nr_1}-e^{-ik_nr_1})/2i$, we see that only the $e^{-ik_nr_1}$ term gives a stationary point. Defining $g(r)=K\rho-k_nr$, the condition for a stationary point is

$$g'(r_1)\equiv\frac{d}{dr_1}\,(K(r_1^2+r_1^2)^{1/2}-k_nr_1)=0=K\frac{r_1}{\rho}-k_n=p_n\frac{r_1}{r_2}-k_n, \tag{39}$$

where $K^2=k_n^2+p_n^2$. Note that the condition for a stationary point is

$$\frac{r_1^{\rm st}}{r_2}=\frac{k_n}{p_n}. \tag{40}$$

If we set $r_2=L$, then there will be one stationary point for $k_n \leqslant p_n$, since r_1 is restricted to lie between 0 and L. For $k_n>p_n$, there is no stationary point, and the integral tends to zero. This is precisely the result we have found in our numerical experiments. Equation (40) also shows that by making $r_2>L$, the integral will tend to zero for values of $k_n<K/\sqrt{2}$ and for $r_2<L$, the integral will be nonvanishing for $k_n>K/\sqrt{2}$, just as we found in our model problem.

Evaluating $g(r_1)$ and $g''(r_1)$ at the stationary point gives

$$g(r_1^{\rm st})=K\rho-k_n r_1^{\rm st}=p_n r_2 \tag{41}$$

and

$$g''(r_1^{\rm st})=\frac{K}{\rho}-\frac{K r_1^{\rm st^2}}{\rho^3}=\frac{k_2^2}{K\rho}. \tag{42}$$

The stationary phase value for the integral is thus

$$I_n=\begin{cases} e^{i3\pi/4}\left(\dfrac{\pi}{p_n L}\right)^{1/2} f(K,\alpha_0)\dfrac{e^{ip_n r_2}}{\sqrt{p_n}}, & r_1^{\rm st}<L \\ \dfrac{1}{2}\,e^{i3\pi/4}\left(\dfrac{\pi}{p_n L}\right)^{1/2} f(K,\alpha_0)\dfrac{e^{ip_n r_2}}{\sqrt{p_n}}, & r_1^{\rm st}=L, \quad \alpha_0=\tan^{-1}\left(\dfrac{k_n}{p_n}\right) \\ 0, & r_1^{\rm st}>L. \end{cases} \tag{43}$$

Using Eq. (36) to evaluate the cross section, with the continuum quadrature weight given by Eq. (32), gives the anticipated result

$$\frac{d\sigma^{\rm st}}{d\varepsilon_n}=\begin{cases} \dfrac{|f(K,\alpha_0)|^2}{k_n p_n}, & r_1^{\rm st}<L \\ \dfrac{|f(K,\alpha_0)|^2}{4k_n p_n}, & r_1^{\rm st}=L \\ 0, & r_1^{\rm st}>L. \end{cases} \tag{44}$$

We have thus established that if we set the value of r_2, which would correspond to the ''unbound'' electron coordinate in a CC treatment, equal to the box length L, which confines the other electron coordinate, and take the limit $L\rightarrow\infty$, then the projection of the exact wave function onto single-particle continuum states gives the exact SDCS for $k_1<k_2$. We obtain one-fourth the correct value when $k_1=k_2$, and zero otherwise. For the model problem results shown in Fig. 6, the energies at which the stationary point lies at $r_1=L$ are indicated for the three different values of r_2 we considered. At these points, the computed cross sections are exactly one-fourth of the exact values, as predicted by Eq. (44).

The result we have derived is valid for any case involving short-range interactions, and not just the simple test case we considered earlier, since the stationary-phase argument we used only depends on the scattered wave function behaving asymptotically as $f(K,\alpha)e^{iK\rho}/(K\rho)^{1/2}$. In fact, we can use the same line of reasoning to derive the identical result for the full six-dimensional wave function, without reference to partial waves. We sketch the argument below.

For short-range potentials, the asymptotic form of the wave function when both coordinates are large is

$$\Phi(\mathbf{r}_1,\mathbf{r}_2)\underset{\rho\rightarrow\infty}{\rightarrow}\left(\frac{K}{2\pi}\right)^{3/2} f(\hat{\mathbf{r}}_1,\hat{\mathbf{r}}_2;K,\alpha)e^{iK\rho}/\rho^{5/2}. \tag{45}$$

We consider the result of projecting such a function onto a single-particle scattering state,

$$I\equiv\left(\frac{K}{2\pi}\right)^{3/2}\int d\hat{\mathbf{r}}_1\int_0^L r_1^2 dr_1 \chi_{\mathbf{k}_1}^{-}{}^{*}(r_1) f(\hat{\mathbf{r}}_1,\hat{\mathbf{r}}_2;K,\alpha)e^{iK\rho}/\rho^{5/2}, \tag{46}$$

where the integration in $\mathbf{r}_1$ is over a sphere of radius L. We use incoming wave boundary conditions for the single-particle state, so the function that appears under the integral in Eq. (46) has the asymptotic form

$$\chi_{\mathbf{k}_1}^{-}{}^{*}(r)\rightarrow e^{-i\mathbf{k}_1\cdot\mathbf{r}}+f(k_1\hat{r})^{*}e^{ik_1 r}/r. \tag{47}$$

To do the integral by stationary phase, we use the asymptotic form of a plane wave [30]:

$$e^{-i\mathbf{k}\cdot\mathbf{r}}\rightarrow\frac{2\pi}{ikr}\left(e^{ikr}\delta(\hat{k}+\hat{r})-e^{-ikr}\delta(\hat{k}-\hat{r})\right). \tag{48}$$

We see that only the incoming part, e^{-ikr} of the plane-wave piece of χ^{-} contributes a stationary point to the integral in Eq. (46). The condition for a stationary point is thus identical to the case we previously considered. If we set $r_2=L$, Eqs. (40)–(42) can be used to derive the result

$$I\underset{L\rightarrow\infty}{\rightarrow}\begin{cases} e^{i3\pi/4}f(\mathbf{k}_1,\mathbf{k}_2;K)e^{ik_2 L}/r_2, & k_1<k_2 \\ \dfrac{e^{i3\pi/4}}{2}\,f(\mathbf{k}_1,\mathbf{k}_2;K)e^{ik_2 L}/r_2, & k_1=k_2 \\ 0, & k_1>k_2, \end{cases} \tag{49}$$

where $k_1^2+k_2^2=K^2$. There are no formal problems with using asymptotic forms for the wave functions in the derivation, since the stationary point r_1^{st} will be large when r_2 and L are both taken to infinity. We have thus established that the ''step-function hypothesis'' holds in the general case, at least for non-Coulomb interactions.

VII. DISCUSSION

Recent attempts to use two-body close-coupling formalisms to calculate differential ionization cross sections have yielded results that are inconsistent with the symmetrization postulate of formal ionization theory. The SDCS values appear to oscillate about the correct result until the ejected electron energy reaches half the maximum available energy, at which point the cross sections go rapidly to zero. A step-function hypothesis has recently been proposed to explain this curious behavior. In this paper, we have attempted to show that the origin of this anomaly is not necessarily in the wave function itself but rather is connected to the way in which the cross section is calculated from the wave function. To support this conclusion, we have performed calculations on the Temkin-Poet model as well as several model problems that do not involve Coulomb potentials. We have also used a stationary-phase argument, which we believe to be valid for any case involving short-range potentials, to explain the observed findings.

There are two aspects of the present work that warrant further comment. One concerns Coulomb interactions. While we believe that the step-function anomaly has no specific connection to the use of long-range Coulomb interactions, we have to concede that we have only been able to explain the oscillations in the singlet Temkin-Poet case through numerical demonstrations. We have not been able to extend the stationary-phase argument we outlined for short-range potentials to the three-body Coulomb case. Therefore, we are still unable to show that the relative angular distributions (doubly and triply differential ionization cross sections) computed by close-coupling methods should converge in the limit of a complete L^2 basis, or to what extent the results depend on the complicated three-body asymptotic phase structure that characterizes the true wave function [15]. If the stationary-phase argument we just outlined for the full wave function in the case of short-range potentials also applied to the Coulomb case, it might indeed explain Bray's [18] observation that, at a particular energy, the error in a CCC calculation is fixed (albeit unknowable) once a particular choice is made for the pseudostate basis and that this error is independent of the partial wave.

The second point is that our treatment differs from ''convergent close coupling,'' in that we used box-normalized target states and matched our projected wave function to an outgoing two-body channel function at a particular value of r_2. The ''step discontinuity'' at $E/2$ results when that matching point is made equal to the box length. In that respect, our treatment is closer to the *R*-matrix plus pseudostate (RMPS) method [31], in which the full wave function is expanded inside a box and then matched at its surface to a sum of energetically open two-body channel functions. However, both the RMPS and CCC methods have shown the same behavior when applied to the Temkin-Poet model [8], and that behavior is reproduced in our numerical experiments. Evidently, the discretization of the continuum that takes place in the CCC method also implies a sort of ''box'' which confines the target states.

While we believe we have discovered the origin of the step-function anomaly, we have unfortunately not shown a way to avoid it in close-coupling calculations. The singly differential cross sections may converge in the limit of a complete L^2 basis for the discretized continuum motion, but they clearly do so much more slowly than the total ionization cross section. The only instances in which the SDCS extracted from a CC wave function appear to converge rapidly are those in which it is vanishingly small at $E/2$. For real ionization problems, this only occurs at high collision energies or for specific symmetry components (such as the triplet total $L=0$ case in *e*-H ionization) which constitute only a small portion of the observed cross section. At lower energies, the amplitude of the oscillations can have the same order of magnitude as the desired cross sections, which would make it difficult to obtain accurate information about the SDCS in a case where its general features are not already known. By the same token, if the wave functions themselves, and not just the two-body scattering amplitudes, are available from a CC calculation, then a direct evaluation of the ionization flux at finite ρ_0 followed by extrapolation might provide a stable alternative for extracting the desired information.

ACKNOWLEDGMENTS

This work was performed under the auspices of the U.S. Department of Energy by the Lawrence Livermore National Laboratory and the Lawrence Berkeley National Laboratory under Contract Nos. W-7405-Eng-48 and DE-AC03-76SF00098.

[1] I. C. Percival and M. J. Seaton, Proc. Cambridge Philos. Soc. **53**, 654 (1957).
[2] P. G. Burke, D. F. Gallaher, and S. Geltman, J. Phys. B **2**, 1142 (1969).
[3] P. G. Burke and J. F. B. Mitchell, J. Phys. B **6**, 320 (1973).
[4] D. H. Oza and J. Callaway, Phys. Rev. A **27**, 2840 (1983); D. H. Oza, Phys. Rev. A **30**, 1101 (1984).
[5] I. Bray and A. T. Stelbovics, Phys. Rev. Lett. **69**, 53 (1992); **70**, 746 (1993).
[6] D. F. Gallaher, J. Phys. B **7**, 362 (1974).
[7] I. Bray, Phys. Rev. Lett. **73**, 1088 (1994).
[8] K. Bartschat and I. Bray, Phys. Rev. A **54**, R1002 (1996).
[9] D. A. Konovalov, I. Bray, and I. E. McCarthy, J. Phys. B **27**, L413 (1994).
[10] See, for example, P. W. Langhoff, in *Electron-Molecule and Photon-Molecule Collisions*, edited by T. N. Rescigno, B. V. McKoy, and B. I. Schneider (Plenum, New York, 1979), p. 183.
[11] E. J. Heller, T. N. Rescigno, and W. P. Reinhardt, Phys. Rev. A **8**, 2946 (1973).
[12] B. H. Bransden and A. T. Stelbovics, J. Phys. B **17**, 1877 (1984).

[13] I. Bray, D. A. Konovalov, I. E. McCarthy, and A. T. Stelbovics, Phys. Rev. A **50**, R2818 (1994); I. Bray and D. V. Fursa, J. Phys. B **28**, L435 (1995).
[14] I. Bray and D. Fursa, Phys. Rev. Lett. **76**, 2674 (1996).
[15] M. Rudge, Rev. Mod. Phys. **40**, 564 (1968).
[16] I. Bray and D. Fursa, Phys. Rev. A **54**, 2991 (1996).
[17] G. Bencze and C. Chandler, Phys. Rev. A **59**, 3129 (1999).
[18] I. Bray, Phys. Rev. Lett. **78**, 4721 (1997).
[19] A. Temkin, Phys. Rev. **126**, 130 (1962); R. Poet, J. Phys. B **11**, 3081 (1978).
[20] M. Baertschy, T. N. Rescigno, W. A. Isaacs, and C. W. McCurdy, Phys. Rev. A **60**, R13 (1999).
[21] C. W. McCurdy, T. N. Rescigno, and D. Byrum, Phys. Rev. A **56**, 1958 (1997).
[22] B. Simon, Phys. Lett. A **71**, 211 (1979).
[23] N. Miyashita, D. Kato, and S. Watanabe, Phys. Rev. A (to be published).
[24] J. V. Lill, G. A. Parker, and J. C. Light, Chem. Phys. Lett. **89**, 483 (1982).
[25] D. E. Manolopoulos and R. E. Wyatt, Chem. Phys. Lett. **152**, 23 (1988).
[26] I. Bray and A. T. Stelbovics, At. Data Nucl. Data Tables **58**, 67 (1994).
[27] C. W. McCurdy and T. N. Rescigno, Phys. Rev. A **56**, R4369 (1997).
[28] E. Gerjuoy, Philos. Trans. R. Soc. London **270**, 197 (1971).
[29] E. T. Copson, *Asymptotic Expansions*, (Cambridge University Press, Cambridge, England, 1967).
[30] A. Messiah, *Quantum Mechanics*, (Wiley, New York, 1966), Vol. II, p. 871.
[31] K. Bartschat, E. T. Hudson, M. P. Scott, P. G. Burke, and V. M. Burke, Phys. Rev. A **54**, R998 (1996).